Chin. J. Astron. Astrophys. Vol. 6 (2006), No. 3, 345–353
(*http://www.chjaa.org*)

Chinese Journal of
Astronomy and
Astrophysics

The Filament Eruption of 1999 March 21 and Its Associated Coronal Dimmings and CME *

Yun-Chun Jiang, Le-Ping Li and Li-Heng Yang

National Astronomical Observatories/Yunnan Observatory, Chinese Academy of Sciences, Kunming 650011; *jyc@ynao.ac.cn*

Received 2005 August 4; accepted 2006 March 31

Abstract We report a filament eruption near the center of the solar disk on 1999 March 21, in multi-wavelength observations by the *Yohkoh* Soft X-Ray Telescope (SXT), the Extreme-ultraviolet Images Telescope (EIT) and the Michelson Doppler Imager (MDI) on the *Solar and Heliospheric Observatory* (SOHO). The eruption involved in the disappearance of an Hα filament can be clearly identified in EIT 195 Å difference images. Two flare-like EUV ribbons and two obvious coronal dimming regions were formed. The two dimming regions had a similar appearance in lines formed in temperature range 6×10^4 K to several 10^6 K. They were located in regions of opposite magnetic polarities near the two ends of the eruptive filament. No significant X-ray or Hα flare was recorded associated with the eruption and no obvious photospheric magnetic activity was detected around the eruptive region, and particularly below the coronal dimming regions. The above surface activities were closely associated with a partial halo-type coronal mass ejection (CME) observed by the Large Angle and Spectrometric Coronagraphs (LASCO) on the SOHO. In terms of the magnetic flux rope model of CMEs, we explained these multiple observations as an integral process of large-scale rearrangement of coronal magnetic field initiated by the filament eruption, in which the dimming regions marked the evacuated feet of the flux rope.

Key words: Sun: activity — Sun: filaments — Sun: coronal mass ejections(CMEs) — Sun: magnetic fields

1 INTRODUCTION

Coronal mass ejections (CMEs) are sudden eruptions of solar plasma and magnetic fields into interplanetary space. They represent large-scale rearrangement of the coronal magnetic fields and are considered to be the key causal link between solar activity and major transient interplanetary and geomagnetic storms. Halo CMEs, diffuse ring-like clouds appearing beyond the edge of the occulting disk, when Earth-directed, can lead to major disturbances of the Earth's magnetic field, hence their importance from the viewpoint of space weather. Observations of early on-disk CME signatures are thus important in identifying such CMEs and in understanding the ultimate driving mechanism of CMEs. Previous observations have shown that CMEs were closely associated with solar flares, eruptions of filaments and coronal sigmoidal structures, as well as attendant phenomena (Hudson & Cliver 2001). Some Earth-directed CMEs, however, only had very weak surface signatures of eruptive solar activity (Švestka 2001): they did not have any associated flare or minor

* Supported by the National Natural Science Foundation of China.

visible chromospheric activity, yet they led to the most important geomagnetic effects (Webb et al. 1998; McAllister et al. 1996). In these cases, detection of other on-disk coronal signatures of Earth-directed CMEs is of great value in space weather prediction.

Recently, coronal dimmings have been identified as the on-disk CME proxy in halo events with observations from the *Yohkoh* Soft X-ray Telescope (SXT) and *Solar and Heliospeheric Observatory* Extreme Ultraviolet Telescope (SOHO/EIT) (Thompson et al. 1998; Wang et al. 2000; Thompson et al. 2000). Since typical timescales of the coronal dimmings, from an hour to several days, are shorter than that of radiation in the corona, they are often explained as resulting from a density drop rather than a temperature decrease (Hudson & Webb 1997). Especially, as good indicators of major coronal disturbances, the so-called bipolar double dimmings in association with eruptions of filaments or X-ray sigmoid structures have been regarded as key signatures of CMEs and attracted a great deal of attention (Sterling et al. 1997; Zarro et al. 1999; Jiang et al. 2003). It is believed that bipolar double dimmings represent the footprints of large-scale flux rope ejections and a loss of the coronal mass sweeping into the CME.

On 1999 March 21, a filament eruption not associated with any GOES and Hα flares occurred around NOAA Active Region 8494 near the disk center. Two coronal dimming regions were formed during this eruption and a partial halo CME was observed by the Large Angle and Spectrometric Coronagraphs on SOHO (SOHO/LASCO). In this paper, we present soft X-ray, EUV, Hα and photospheric magnetic field observations of this event, and will show that the CME was directly associated with the weak eruption and the coronal dimmings, which can be regarded as its clear on-disk proxy.

2 OBSERVATIONS

For the present study, the following data are used.

(1) Full-disk Hα images accessible through the Internet. The Hα heliograms of the Kanzelhöhe Solar Observatory (KSO) and the Big Bear Solar Observatory (BBSO) are used to search for the disappeared filament.
(2) SOHO/EIT full-disk EUV 195 Å (FeXII, 1.5 $\times$ 10^6 K), 171 Å (Fe IX/X, 1$\times$ 10^6 K), 284 Å (Fe XV, 2$\times$ 10^6 K) and 304 Å (He II, 6$\times$ 10^4 K) images (Delaboudiniére et al. 1995). On 1999 March 21, EIT continuously obtained 195 Å images roughly every 12 minutes with a pixel resolution of $2.6''$, while 171 Å, 284 Å and 304 Å images were taken once every 6 hours.
(3) Yohkoh/SXT full-disk soft X-ray images in the wavelength range of 3–50 Å (2–4 $\times$ 10^6 K) with a variable cadence and a pixel resolution of $4.9''$ (Tsuneta et al. 1991).
(4) C2 and C3 white-light coronagraph data from SOHO/LASCO, which respectively cover the range of 2 to 6 and 4 to 32 solar radii (Brueckner et al. 1995).
(5) SOHO/MDI full-disk line-of-sight magnetograms with a pixel size of $2''$ and a cadence of 1 minute (Scherrer et al. 1995). For the present study, the MDI full-disk intensity images are also examined.

3 RESULTS

The eruptive filament was located at the southern boundary of NOAA Active Region 8494, a small decaying active region of small sunspots near its central meridian passage on March 21 (S23W03). The filament erupted between 12:35 and 14:30 UT. Figure 1a and 1b present Hα line center and soft X-ray images before and after the eruption. We see that the Hα filament that appeared at 11:31 UT (indicated by the two white arrows), was no longer seen by 15:48 UT. As common features of Hα filament eruptions, post-eruptive coronal loops in soft X-ray (labelled "PEL") appeared at 15:05 UT, which span the whole Hα filament channel, and two coronal dimming regions ("D1" and "D2") seemed to appear near the two ends of the erupted filament.

The most complete observations covering the whole event under consideration were made by SOHO/EIT at the 195 Å wavelength. In the original EIT 195 Å observations, the EUV counterpart of the Hα filament was quite ambiguous, barely showing the eruptive process. However, the eruption is evident in 195 Å running difference image (see Fig. 2). It is clear that a slow eruption towards the southwestern direction (indicated by the thick black arrows) indeed occurred between about 12:35 to 14:30 UT. Moreover, by examining the direct EIT 195 Å images (Fig. 3a) and the difference images after subtracting a pre-event

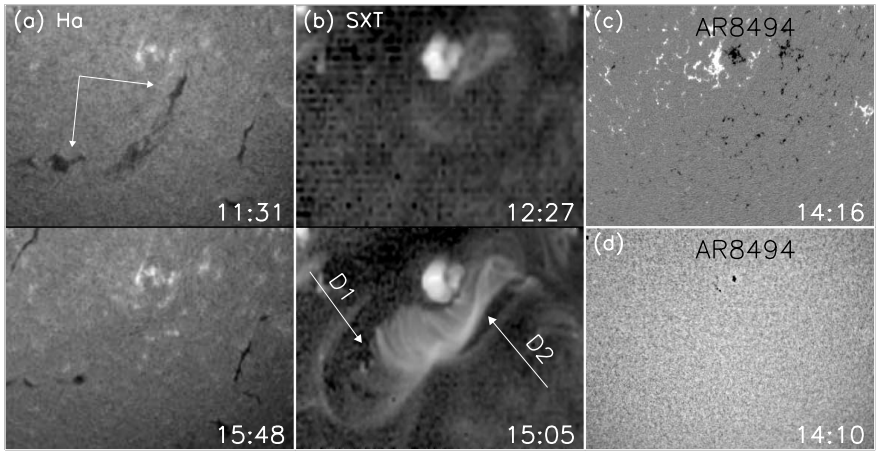

Fig. 1 Hα line center (a) and SXT soft X-ray (b) images of 1999 March 21 illustrating disappearance of the filament, MDI line-of-sight magnetogram (c), and continuum intensity image (d), showing magnetic configuration of the eruptive region. After the filament eruption, two coronal dimming regions, D1 and D2, appeared around the two ends of the eruptive filament. The field of view (FOV) is $860'' \times 740''$.

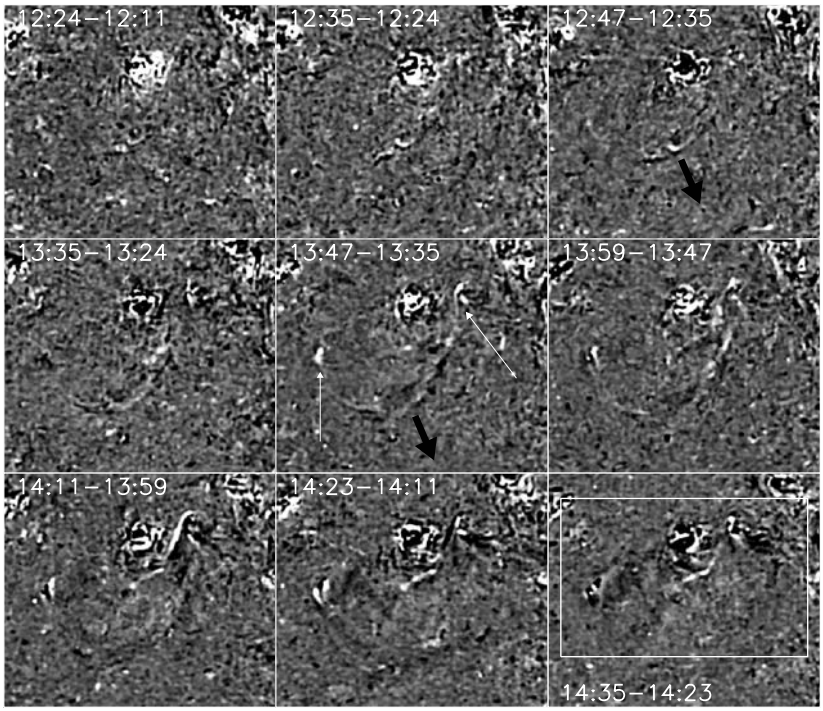

Fig. 2 EIT 195 Å running difference images showing the filament eruption. The FOV is the same as in Figure 1.

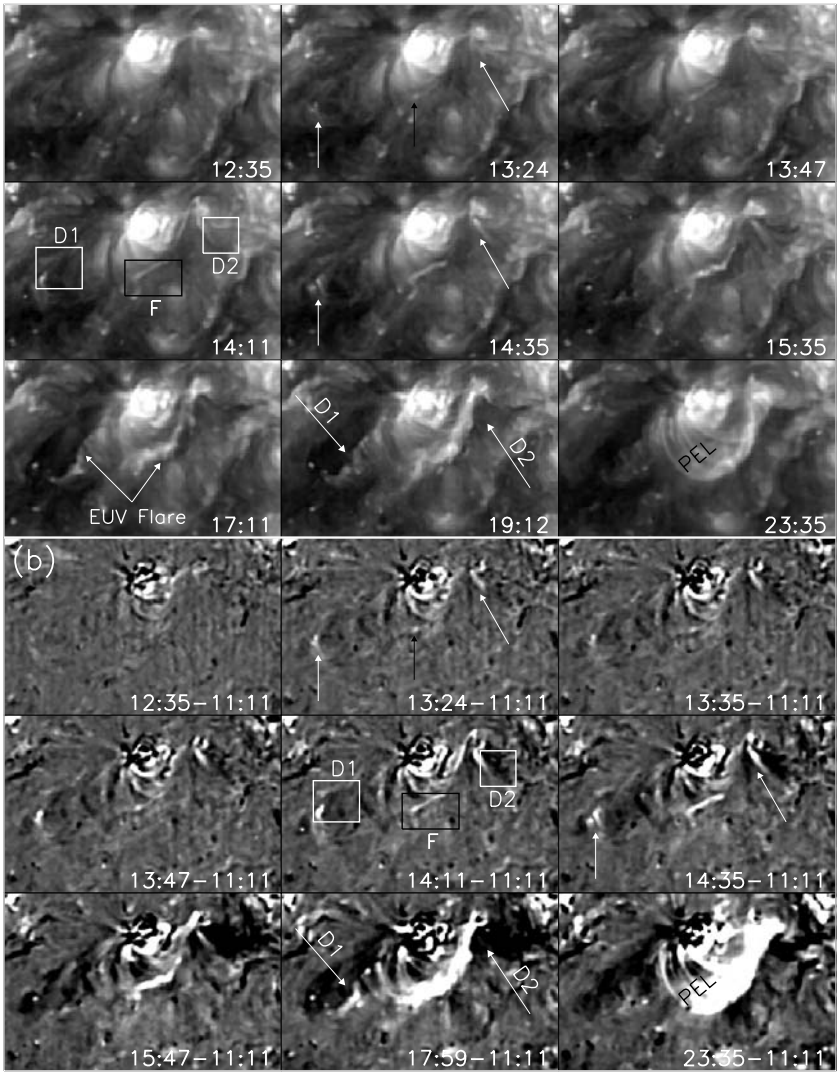

Fig. 3 EIT 195 Å original images (a) and difference images (b) showing the evolution of the event. To clearly exhibit the formation of the coronal dimmings, the difference images are obtained by subtracting the 11:11 UT image from the image at a given time in each case. The FOV, indicated by the white box in Fig. 2, is $780'' \times 500''$.

image (Fig. 3b), we found many features characteristic of Hα filament eruptions. First, the eruption was accompanied by the appearance of two EUV flare-like ribbons on opposite sides of the eruptive filament (indicated by the two white arrows in 195 Å images at 17:11 UT in Fig. 3a). Secondly, EUV post-eruptive loops, PEL, gradually appeared to connect the two ribbons. Their footpoints coincided with the EUV ribbons in location so their expansion was concurrent with the increasing separation of the EUV ribbons. Finally, the MDI magnetograms showed that the two EUV ribbons were located above the regions of opposite magnetic polarities (see Fig. 1c and Fig. 4a).

As shown in Figure 1a, weak Hα enhancements appeared around the site of the filament after the eruption. Unfortunately, only one Hα image from KSO was available before the eruption, while the earliest

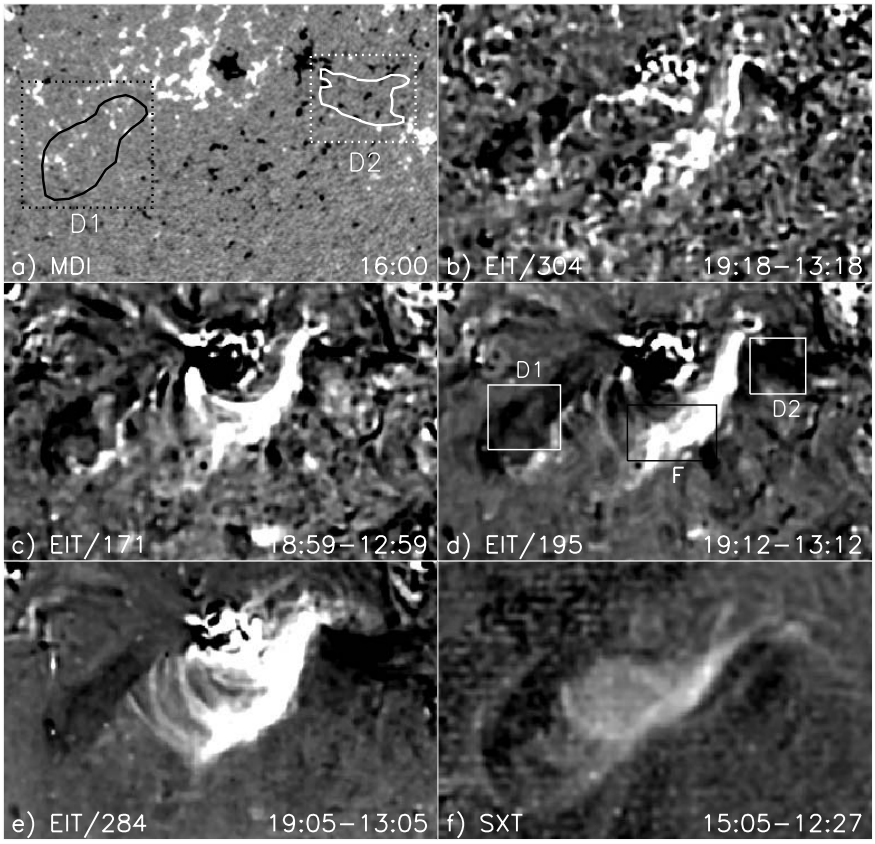

Fig. 4 MDI line-of-sight magnetogram (a), EIT 304 Å (b), 171 Å (c), 195 Å (d), 284 Å (e) and SXT soft X-ray (f) difference images. The two coronal dimming regions, D1 and D2, are located on the regions of opposite magnetic polarities and are superposed as black and white contours in (a). The FOV is the same as in Fig. 3.

BBSO Hα observation was from 15:48 UT on, i.e., after the eruption. Thus, we can not examine the evolution of these Hα enhancements. However, no optical flare was reported by the Solar Geophysical Data online around the time of the event, possibly indicating that the Hα enhancements were too weak to be regarded as an Hα flare. Moreover, GOES did not register the event as a flare. The GOES 1–8 Å soft X-ray flux profile is plotted in Figure 6a. Beginning at 14:43 UT (indicated by the arrow in Fig. 6a), the GOES soft X-ray flux showed a weak increase relative to the background level and then contained the signature of a long duration event to about 20:00 UT. However, the event peaked below X-ray class B1 level and so no GOES flare was recorded after the beginning of the EUV flare. Thus, only minor chromospheric and GOES X-ray activities were involved in the global coronal restructuring resulting from the filament eruption.

As mentioned above and shown in Figure 1b, two coronal dimming regions (D1 and D2) were formed during the eruption. In the EIT 195 Å direct and difference images shown in Figure 3, the formation of the two coronal dimmings can be clearly detected in the time of the EUV ribbons. It is very interesting to note that EUV brightenings first appeared in the interior of the dimmings, then gradually faded away and were eventually replaced by darkening. The appearances of the EUV brightenings are clear in the 195 Å direct and difference images of Figures 2 and 3 (indicated by the white arrows in Figure 2, and in the images at 13:24 and 14:35 UT in Figs. 3a and 3b). In Figure 4, we compare the difference images from the pre-event images at 304 Å, 171 Å, 195 Å, 284 Å and soft X-ray. These lines are formed in temperature range from 6

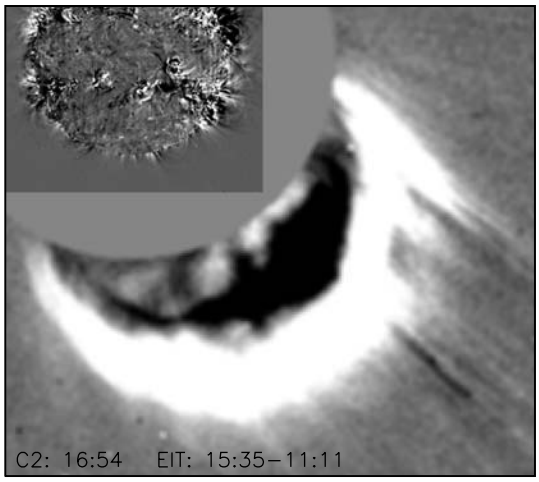

Fig. 5 Combination of the inner EIT 195 Å with the outer LASCO C2 difference images.

$\times 10^4$ K to several 10^6 K; in these, the two dimmings were obvious and showed a similar shape. Thus, as the finding of Hα dimmings in a halo event (Jiang et al. 2003), D1 and D2 may have counterparts in the chromosphere, i.e., the dimmings may have extended from the corona into the chromosphere. It is a pity that we do not have continuous Hα observations to confirm any dimmings in Hα.

Like bipolar double dimmings in the eruptions of the sigmoid structures and filaments found associated with halo CMEs (Sterling & Hudson 1997; Jiang et al. 2003; Zarro et al. 1999), the MDI magnetograms (see Fig. 4a) showed that the two dimmings were located over regions of opposite magnetic polarities, around the two ends of the erupted filament. Figure 6a also shows the EIT 195 Å light curves in the three boxes in Figures 3 and 4d centered on D1, D2 and one of the EUV flare ribbons, F. We see that around the start time of the weak increase of GOES soft X-ray flux (14:43 UT), there was apparent increase in F and decrease in D1 and D2. We would like to point out that the resulting 195 Å light curve profiles, while dependent on the window used in the intensity measurements, showed similar changing trends. Due to the low temporal resolution of EIT observation and the lack of detailed information on the impulsive phase of the EUV flare, it is difficult to determine the exact onset time of the EUV flare and the dimmings. By carefully examining the base-fixed difference images, it is found that the initial enhancements of the EUV flare could at least be traced back to 13:24 UT (see the black arrows in the images at 13:24 UT in Fig. 3), and the dimmings occurred nearly at the same time (see Fig. 6a). Therefore, the eruption process of the event appears to be that the filament first began to slowly rise at 12:35 UT, then the initial dimmings and brightenings occurred at around 13:24 UT, and the EUV flare eventually started at about 14:43 UT, approximately consistent with the start of soft X-ray flux increase.

Since the instability of a filament is probably related to photosphere activities, such as newly emerging flux, flux cancellation and so on (Moore & Roumeliotis 1992; Feynman & Martin 1995; Wang & Sheeley 1999; Jiang & Wang 2000, 2001; Kim et al. 2001; Liu et al. 2003), we inspected the MDI observations of magnetic field for possible associated magnetic activities in a window well covering the eruption region, but only found slow continuous flux changes. We first examined MIDI magnetograms with a 96-minute cadence over a period of a few days but found no obvious flux emergence inside the region. We then examined MDI magnetograms with a 1-minute cadence for a period of 19 hours spanning the eruption but again found no measurable flux cancellation along the filament channel. From 04:00 to 23:00 UT on March 21, the magnetic fields around the eruption region only showed a slow evolution similar to that of a typical non-flare period. Thus, it seems that any photosphere activity related to the eruption was kept to a low level, consistent with the weak level of surface activities during the event. This finding probably indicates that the filament eruption resulted from the normal slow magnetic evolution in the region. It is interesting to

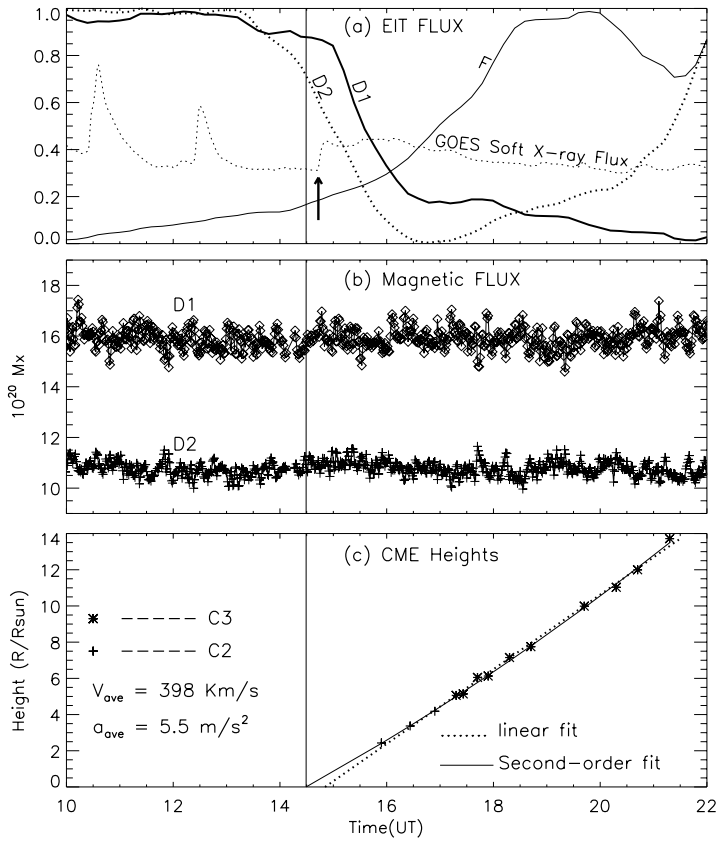

Fig. 6 (a) Time profiles of GOES-8 soft X-ray in the energy channel of 1–8 Å, which is displayed in an arbitrary unit to fit in the panel, and EIT 195 Å light curves as the function of time in the regions centered on the three boxes, 'F', 'D1' and 'D2', in Figures 3 and 4, which are computed from the intensity integrated and normalized over these regions. (b) Changes of the magnetic flux in the two dashed boxes of the magnetogram in Figure 4, which cover the two coronal dimming regions. To improve clarity, we plot the absolute values for the negative flux. (c) Height of the CME front as function of time. The solid vertical bars indicate the extrapolated onset time of the CME by the use of second-order polynomial fitting, and the arrow in the top panel, the start time of the small increase in GOES soft X-ray flux.

note that, although the coronal dimmings may extend into the lower atmosphere, no obvious changes were detected in the photospheric field below. Changes of positive and negative fluxes in two areas including D1 and D2 (indicated by the two dashed boxes in Fig. 4a) were measured and are plotted in Figure 6b. It is clear that the magnetic fluxes below the two dimmings faintly and smoothly changed throughout the eruption period. The magnetic flux of the whole area in the FOV of Figure 4a also showed similar changes. We would like to stress that such result is highly dependent on the limited sensitivity and spatial resolution of the full-disk MDI magnetograph observations.

Along the direction of the filament eruption, a partial halo CME was observed by SOHO/LASCO around the time. Figure 5 is a composite image of an inner EIT 195 Å with an outer LASCO C2 difference image. The CME first appeared in the field of view of the LASCO C2 at 15:54 UT, and later in the LASCO C3 at 17:42 UT, in the form of a large bright loop front extending over the S pole to the SW limb. According to Seiji Yashiro's measurements, its center is at position angle (PA) 208°, and it had a width of 141°.

Its height-time (H-T) plot at PA 194° is shown in Figure 6c. The average speed of the CME front from the linear fitting is 398 km s^{-1}, and the average acceleration from the second-order polynomial fitting, 5.5 m s^{-2}. These parameters (indicated in the low left corner of Fig. 6c) showed that the CME was a slow one, consistent with the results that slow CMEs are more often found associated with filament eruptions (Sheeley et al. 1999; St. Cyr et al. 2000). By applying second-order (first-order) polynomial fitting, back extrapolation of the CME front from the H-T plot to the solar disk center yields an estimate of the onset time of the CME at about 14:29 UT (14:51 UT), which is very close to the start time of the GOES soft X-ray flux increase (14:43 UT). Although an accurate estimate of the onset time of the CME is difficult due to lacking of necessary information of the CME dynamics at its early stage (Zhang et al. 2001), the above spatial and temporal consistency suggests that the filament eruption, the following coronal dimmings and EUV flare were directly associated with the CME initiation. It is noted that occurrence of the earliest dimmings and brightenings of the EUV flare were nearly at the same time (13:24 UT), which was before the extrapolated CME onset. This possibly indicates that the CME had an initiation phase before its impulsive acceleration phase (Zhang et al. 2004), resulting from the slow rise of the eruptive filament before the EUV flare onset (Sterling & Moore 2003, 2004).

4 CONCLUSIONS AND DISCUSSION

An Hα filament erupted near the center of the solar disk on 1999 March 21. In this paper we present a detailed study on the eruption and the associated coronal dimmings and CME, as well as the evolution of photospheric magnetic fields in the eruption region. The main results are as follows. (1) The disappearance of Hα filament involved the faint Hα enhancements, the two EUV flare ribbons, the two coronal dimmings and the post-event coronal loops, but was not associated with any significant X-ray flare or Hα flare. The changes of the photospheric magnetic field in the eruption region were slow and smooth; no obvious flux emergence and cancellation were detected in the filament channel during the eruption. (2) A bipolar double dimming (D1 and D2) formed in the regions of opposite magnetic polarities near the two ends of the erupted filament. The dimming started nearly at the same time as the initial brightenings of the EUV flare and clearly appeared in lines formed in the temperature range 6×10^4 K to several 10^6 K. However, no changes of photospheric magnetic field were detected below and around them. (3) The filament eruption showed a close spatial and temporal relationship with the partial halo CME. It appears that the two dimmings were a good indicator of the on-disk source region of the CME.

It is not uncommon that an Hα filament eruption can be regarded as a clear on-disk CME proxy. However, an important aspect of the March 21 event is that the filament eruption was slow and unimpressive, and was not associated with any Hα and GOES flare. Thus, it will be difficult to directly relate such weak solar activity to the partial halo CME only according to the traditional surface CME signatures. Owing to the formations of the two coronal dimmings, we can pay attention to this eruption and find out that these dimmings were the on-disk indicative of the CME source regions. Although the chromosphere activity responding to the filament disappearance was too faint to be called as an Hα flare, the flare-like properties at 195 Å (see Zhou, Wang & Cao 2003), i.e., the two EUV flare ribbons and the postevent coronal loops, indeed indicated the occurrence of some major coronal disturbance. Similar examples of weak surface activities associated with CMEs or geomagnetic storms were also well studied by Webb et al. (1998) for the 1997 January 6 on-disk event, by McAllister et al. (1996) for the 1994 April 14 on-disk event, and more recently, by Shakhovskaya et al. (2002) for the 2000 August 11 limb event. These events clearly showed that major coronal perturbation in association with CME may or may not correspond to obvious activity in the chromosphere (Švestka 2001). In these cases, the coronal observations, such as those made by the YOHKOH/SXT and SOHO/EIT, are of great importance in identifying the on-disk CME proxy when there is a lack of clear signature of GOES flares and chromosphere activity.

According to the view that Hα filament is a chromospheric sign for a flux rope system, the eruptive phenomena mentioned above can be understood to be an integral process in the flux rope model of CME, in which the coronal double dimmings mark the evacuated feet of the magnetic flux rope (Streling & Hudson 1997; Zarro et al. 1999; Jiang et al. 2003). The obvious appearances of 304 Å dimmings possibly indicate that the evacuated feet of the flux rope were deeply extended into the chromosphere, and also suggest that the dimmings were due to a density loss rather than a temperature decrease in the coronal plasma. Otherwise, 304 Å brightenings would be observed as the 10^6 K plasma cooled through 6×10^4 K. Therefore, the

dimmings very likely tracked the mass loss that provided mass supply to the CME, which had a relatively large temperature range, from about 6×10^4 K to several 10^6 K.

On the other hand, density reduction was probably involved in the evaporation of chromosphere material heated by the EUV flare since there were brightenings appearing in their interior at the very initial phase of the EUV flare (Yokoyama & Shibata 2001; Chen et al. 2002; Chen, Fang & Shibata 2005). Finally, we would like to point out that we failed to detect obvious changes of photospheric magnetic fields below the two dimmings in the MDI full-disk magnetograms. Since the coronal bipolar double dimmings quite possibly represent the evacuated, deeply rooted feet of the eruptive flux rope system, it is reasonable to expect that measurable changes of photospheric magnetic fields should occur below the dimming regions during their formation. Magnetic field observations with higher sensitivity and spatial resolution are needed to clarify this issue.

Acknowledgements We thank an anonymous referee for many constructive suggestions. We are indebted to the YOHKOH team, the EIT, LASCO and MDI teams for data support. We thank H. D. Chen and S. L. Ma for stimulating discussions and useful comments. The work is supported by the NSFC under Grants 10573033 and 10173023.

References

Brueckner D. E., Howard R. A., Koomen M. J. et al., 1995, Sol. Phys., 162, 357
Chen P. F., Wu S. T., Shibata K., Fang C., 2002, ApJ, 572, L99
Chen P. F., Fang C., Shibata K., 2005, ApJ, 622, 1202
Delaboudiniére J. -P., Artzner G. E., Brunaud J. et al., 1995, Sol. Phys., 162, 291
Feynman J., Martin S. F., 1995, J. Geophys. Res., 100, 3355
Hudson H. S., Webb D. F., 1997, In: N. Crooker, J. Joselyn, J. Feynman, eds., Coronal Mass Ejections, Geophysical Monograph 99; Washington: Am. Geophys. Union, p.27
Hudson H. S., Cliver E. W., 2001, J. Geophys. Res., 106, 25199
Jiang Y., Wang J., 2000, A&A, 356, 1055
Jiang Y., Wang J., 2001, A&A, 367, 1022
Jiang Y. C., Ji H. S., Wang H. M. et al., 2003, ApJ, 597, L161
Kim J., Yun H. S., Lee S. et al., 2001, ApJ, 547, L85
Liu Y., Jiang Y. C., Ji H. S. et al., 2003, ApJ, 593, L137
McAllister A. H., Dryer M., McIntosh P. et al., 1996, J. Geophys. Res., 101, 13497
Moore R. L., Roumeliotis G., 1992, In: Z. Sŭvestka, B. V. Jackson, M. E. Machado, eds., Eruptive Solar Flares, IAU Colloq. 133, Springer–Verlag, p.6
Scherrer P. H., Bogart R. S., Bush R. I. et al., 1995, Sol. Phys., 162, 129
Shakhovskaya A. N., Abramenko V. I., Yurchyshyn V. B., 2002, Sol. Phys., 207, 369
Sheeley N. R., Jr., Walters H., Wang Y.-M. et al., 1999, J. Geophys. Res., 104, 24739
St. Cyr, O. C., Howard R. A., Sheeley N. R. et al., 2000, J. Geophys. Res., 105, 8169
Sterling A. C., Hudson H. S., 1997, ApJ, 491, L55
Sterling A. C., Moore R. L., 2003, ApJ, 599, 1418
Sterling A. C., Moore R. L., 2004, ApJ, 602, 1024
Švestka Z., 2001, Space Sci. Rev., 95, 135
Thompson B. J., Plunkett S. P., Gurman J. B. et al., 1998, Geophys. Res. Lett., 25, 2465
Thompson B. J., Cliver E. W., Nitta N. et al., 2000, Geophys. Res. Lett., 27, 1431
Tsuneta S. T., Acton L., Bruner M. et al., 1991, Sol. Phys., 136, 37
Wang H. M., Goode P. R., Denker C. et al., 2000, ApJ, 536, 971
Wang Y. -M., Sheeley N. R., 1999, ApJ, 510, L157
Webb D. F., Cliver E. W., Gopalswamy N. et al., 1998, Geophys. Res. Lett., 25, 2469
Yokoyama T., Shibata K., 2001, ApJ, 549, 1160
Zarro D. M., Sterling A. C., Thompson B. J. et al., 1999, ApJ, 520, L139
Zhang J., Dere K. P., Howard R. A. et al., 2001. ApJ 559, 452
Zhang J., Dere K. P., Howard R. A. et al., 2004. ApJ 604, 420
Zhou G. P., Wang J. X., Cao Z. L., 2003, A&A, 397, 1057